Journal of Thermal Analysis and Calorimetry, Vol. 55 (1999) 779-788

THERMAL DECOMPOSITIONS OF THE MOLYBDOTELLURATES OF NICKEL(II) AND COBALT(II)

P. A. Lorenzo-Luis[1], *E. R. Castellón*[2], *J. J. Jiménez*[2] *and P. Gili*[1]*

[1]Departamento de Química Inorgánica, Universidad de la Laguna, E-38200 La Laguna Tenerife, Canary Islands
[2]Departamento de Química Inorgánica, Cristalografía y Mineralogía, Facultad de Ciencias Universidad de Málaga, E-29071 Málaga, Spain

(Received April 21, 1998)

Abstract

Molybdotellurates $[M(H_2O)_6]_3[TeMo_6O_{24}]$, with *M*=Ni(II) and Co(II), were synthesized and characterized by single-crystal X-ray diffraction for compound 1 and X-ray powder diffraction for compound 2, EDAX, IR, electronic spectra in the solid phase and in solution, and magnetic properties. Thermogravimetry and differential scanning calorimetry of both compounds revealed a loss of 11 water molecules through an endothermal process with ΔH=800 kJ mol^{-1} for the nickel compound and ΔH=833 kJ mol^{-1} for the cobalt compound. The residual compounds were characterized by chemical analysis, IR and XPS spectroscopy

Keywords: cobalt, dynamic and isothermal methods, kinetics, molybdotellurates, nickel

Introduction

Inorganic metal–oxygen clusters are of great interest in catalysis, supramolecular inorganic chemistry, electron transfer reactions and biological chemistry [1]. One important aspect of the chemistry of these compounds is their thermal behaviour. To the best of our knowledge, no experimental data on the thermal stability of telluromolybdates are available with the exception of diazolium [2, 3] and some transition metal molybdotellurates [4].

In previous work, molybdotellurates of nickel(II) and cobalt(II) of general formula $M_3[TeMo_6O_{24}]\cdot nH_2O$, where *M*=Ni, Co, Mn, Zn and Cu, were prepared and incompletely characterized [4, 5]. These compounds are interesting as active catalysts for the oxidation of olefins to unsaturated aldehydes and acids [4]. In more recent work, we reinvestigated and completed the study of transition metal molybdotellurates [6]. In the present work, we report on a study of the thermal

* Author for correspondence: e-mail: pgili@ull.es; fax:34-92-318461.

1418–2874/99/ $ 5.00
© 1999 Akadémiai Kiadó, Budapest
Akadémiai Kiadó, Budapest
Kluwer Academic Publishers, Dordrecht

stability in the solid phase of molybdotellurates of nickel(II) and cobalt(II), $[Ni(H_2O)_6]_3 \cdot [TeMo_6O_{24}]$ 1 and $[Co(H_2O)_6]_3 \cdot [TeMo_6O_{24}]$ 2, and the determination of kinetic parameters corresponding to the loss of 11 water molecules, using dynamic and isothermal methods in dynamic dinitrogen atmosphere for compound 2.

Experimental

Materials

The starting materials (reagent grade) were obtained commercially and used without further purification.

Preparation of the compounds

The compounds were prepared in accordance with reference [6]. Thus, a suspension of MoO_3 (2 g, 13.9 mmol), $Te(OH)_6$, (2.13 g, 10 mmol) and $NiCO_3 \cdot 2Ni(OH)_2 \cdot 4H_2O$ (5.2 g, 13.9 mmol) for compound 1, or of $2CoCO_3 \cdot 3Co(OH)_2 \cdot 4H_2O$ (7.8 g, 13.9 mmol) for compound 2, was prepared in deionized water (1 l). The suspensions were heated under reflux with stirring for 4 h and adjusted to $pH \approx 2$ by dropwise addition of HNO_3 (13.1 M). The resulting green solution for compound 1 or pink solution for compound 2 was reduced in volume, first to 300 cm^3 with a rotatory evaporator, and then by slow evaporation to 200–150 cm^3 for both compounds at room temperature. Anal. calc. $Ni_3Mo_6O_{42}H_{36}Te$ (1): Ni, 10.90; H, 2.29; Mo, 36.26; Te, 8.03; Found: Ni, 11.20; H, 2.40; Mo; 36.83; Te, 7.96%. Anal. calc. $Co_3Mo_6O_{42}H_{36}Te$ (2): Co, 11.13; H, 2.30; Mo, 36.24; Te, 8.03; Found: Co, 11.74; H, 2.34; Mo, 36.95; Te, 8.20%.

Analytical methods

Chemical analysis of H was performed on an EA 1108 CHNS-O automatic analyser, and EDAX chemical analyses of Ni, Co, Te and Mo were performed with a Philips CM200 transmission electron microscope.

Single-crystal X-ray diffraction data for compound 1 were recorded on an Enraf-Nonius CAD-4 four-circle diffractometer at 293(2) K. Intensity data were obtained by use of an $\omega 2\theta$ scan, using graphite-monochromated CuK_α radiation (λ=1.54169 Å).

X-ray powder diffraction data for compound 2 were collected by using Debye-Sherrer geometry, and a 120° arch detector INEL, with the sample in a rotating capillary to diminish preferred orientation. The radiation was CuK_α (λ=1.5406 Å), using a primary planar graphite monochromator.

IR spectra were recorded on a Nicolet 710 FTIR spectrophotometer, in KBr as support, in the spectral range 4000–250 cm^{-1}. Solid-state electronic spectra were obtained with a Perkin-Elmer 550S spectrophotometer in the spectral range 190–900 nm, with $BaSO_4$ as support, while the spectra in aqueous solution were

recorded on a Perkin-Elmer Lambda 9 spectrophotometer UV-VIS-NIR in the spectral range 300–1300 nm. The magnetic susceptibility data on the powdered samples were obtained with a Quantum Design SQUID MPMS-5S magnetometer in the temperature range 1.7–300 K. Pd and $Hg[Co(SCN)_4]$ were used for calibration.

Thermogravimetric (TG) and calorimetric analyses were performed on a Netzsch STA 409 EP simultaneous thermobalance and a differential scanning calorimeter (DSC), respectively, at heating rates of 2.5 and 8°C min^{-1} in a dynamic dinitrogen atmosphere of ca 70 cm^3 min^{-1} with 5.1 mg of compound. Several runs were made on each sample, with good reproducibility. The instrument was standardized for temperature and ΔH *vs.* five reference materials: KNO_3, In, $KClO_4$, K_2SO_4 and $BaCO_3$.

For determination of the kinetic parameters, thermogravimetric curves and their derivatives were obtained. The residual compounds were characterized by IR and XPS spectroscopy. The XPS spectra were recorded on a Physical Electronics 5700 spectrometer equipped with a dual X-ray excitation source (MgK_α, $h\nu$=1253.6 eV and AlK_α, $h\nu$=1486.6 eV) and an Electronics 80-365B multichannel analyser.

Results and discussion

The compounds $Ni_3[TeMo_6O_{24}]\cdot 20H_2O$ [4] and $Co_3[TeMo_6O_{24}]\cdot 24H_2O$ [5] were earlier precipitated from solutions containing the nitrates of the respective transition metal, telluric acid and ammonium paramolybdate. This method of synthesis is very different from our method of preparation (vide supra) and produces species that are more hydrated than those described in the present work.

The compounds described here were characterized by X-ray diffraction, IR and electronic spectroscopy in the solid state and in aqueous solution and via the magnetic susceptibilities [6]. $[Ni(H_2O)_6]_3\cdot[TeMo_6O_{24}]$ and $[Co(H_2O)_6]_3\cdot[TeMo_6O_{24}]$ crystallize in the trigonal space group R-3c, with a=b=17.906(5), c=19.458(5) Å, V=5403(3) $Å^3$ for 1, and a=b=17.902(4), c=19.686(3) Å, V=5448(2) $Å^3$ for 2. The structure of compound 2 was refined by using the Rietveld method, starting with the structural parameters of the isostructural compound 1. The two compounds are isostructural, because they present the same powder diffractograms under the same conditions. The anion is located around aquo cations $[M(H_2O)_6]^{2+}$ (M=Ni(II); Co(II)). A hydrogen-bonding network allows the self-assembly of the ionic counterparts [6].

The IR spectra of both compounds are discussed on the basis of the D_{3d} symmetry of the anion $[TeMo_6O_{24}]^{6-}$. The bands at 905 and 954 cm^{-1} are assigned to ν_s and ν_{as} of *cis*-MoO_2 (A_{2u}+2E_u), corresponding to the idealized D_{3d} symmetry for $[TeMo_6O_{24}]^{6-}$. The bands at 622 and 692 cm^{-1} could be tentatively assigned to the ν_{as} Te–O stretching mode (A_{2u}+E_u) [2, 6, 7]. The band at 622 cm^{-1} could also correspond to wagging frequencies (ρ_w) of the water molecules in $[M(H_2O)_6]^{2+}$ (M=Ni(II), Co(II)), with idealized O_h symmetry of the cation [8].

The visible spectrum for the nickel compound in aqueous solution presents a band at 393 (ε=2.3 M^{-1} cm^{-1}), a doublet at 660 (ε=0.8 M^{-1} cm^{-1}), and band at 725 (ε=0.9 M^{-1} cm^{-1}) and 1120 nm (ε=0.5 M^{-1} cm^{-1}). These bands correspond to ligand field transitions of the octahedral complex $[Ni(H_2O)_6]^{2+}$, and are assigned to the transitions $^3A_{2g}\rightarrow{}^3T_{1g}(P)$, $^3A_{2g}\rightarrow{}^1E_g$, $^3A_{2g}\rightarrow{}^3T_{1g}(F)$ and $^3A_{2g}\rightarrow{}^3T_{2g}$, respectively. In the solid phase, the doublet is observed at 650 and 715 nm. The visible spectrum for the cobalt compound in aqueous solution presents bands at 475 (ε=17.3 M^{-1} cm^{-1}), 510 (ε=22.7 M^{-1} cm^{-1}) and 605 nm (ε=1.7 M^{-1} cm^{-1}), attributed to the transitions $^4T_{1g}\rightarrow{}^4T_{1g}(P)$ (bands at 475 and 510 nm) and $^4T_{1g}\rightarrow{}^4A_{2g}$ (band at 605 nm) of the ligand field of the octahedral complex $[Co(H_2O)_6]^{2+}$ whereas in the solid phase, bands are observed at 470 and 517 nm [6].

The small nature of the shifts observed in the visible bands in the solid phase with respect to the bands in solution for both complexes seems to indicate that the complexes maintain the same structure in the solid phase as in aqueous solution.

The effective magnetic moment found for the nickel molybdotellurate is 3.10 BM, which is slightly higher than expected for the spin–only contribution of Ni(II) with S=1. This small difference can be explained if it is taken into account that the Ni(II) is coordinated by 6 water molecules in a distorted octahedron. The magnetic moment observed for the cobalt compound is 4.57 BM. This value agrees with that expected for the crystal field ground term $^4T_{1g}$ associated with Co(II) in a point idealized symmetry O_h, for which the orbital contribution should be considered [6].

For both compounds, thermogravimetric analyses were performed between 22 and 600°C, at heating rates of 2, 5 and 8°C min^{-1} in a dynamic dinitrogen atmosphere of ca 70 cm^3 min^{-1}, with 5.1 mg of compound. A clear step was observed, corresponding to the loss of 11 water molecules (calc. mass loss 12.5, found 12.3%) between 73 and 120°C for compound 1 (Fig. 1 and Table 1) and between 58 and 114°C for compound 2 (Fig. 2 and Table 1), according to the equation

$$[M(H_2O)_6]_3{\cdot}[TeMo_6O_{24}]_{(s)} \rightarrow [6MoO_3{\cdot}3MO{\cdot}TeO_3{\cdot}7H_2O]_{(s)} + 11H_2O_{(g)}$$

where M=Ni(II), Co(II), through an endothermic process with ΔH=800 kJ mol^{-1} for compound 1 and ΔH=833 kJ mol^{-1} for compound 2.

The values of ΔH for the water molecules are larger than those obtained for the loss of water molecules from other compounds where the water molecules are bonded by hydrogen-bonds [2, 3].

Compound 2 loses the water molecules (between 58 and 114°C) before compound 1 (between 73 and 120°C), due to the fact that the distortion of the octahedron of $[Co(H_2O)_6]^{2+}$ 2 is greater than that of $[Ni(H_2O)_6]^{2+}$ 1 [6]. This is in accordance with the Irving-Williams series of stability [9].

The residual compounds $[6MoO_3{\cdot}3MO{\cdot}TeO_3{\cdot}7H_2O]$ (M=Ni(II), Co(II)) from the first step, which are green for 1 and brown for 2, displayed thermal stability up to 287°C for compound 1 and to 258°C for compound 2 (Figs 1 and 2, respectively). These compounds were also characterized by IR spectroscopy and ele-

Table 1 TG data obtained at different heating rates for the thermal dehydration of $[Ni(H_2O)_6]_3{\cdot}[TeMo_6O_{24}]$ (compound 1) and $[Co(H_2O)_6]_3{\cdot}[TeMo_6O_{24}]$ (compound 2)

	2°C min^{-1}			5°C min^{-1}			8°C min^{-1}		
	T_i	T_f	T_s	T_i	T_f	T_s	T_i	T_f	T_s
1	73	110	94	73	118	109	74	120	115
2	58	100	77	58	111	87	58	114	88

T_i and T_f are the initial and final temperatures of reaction, respectively, whereas T_s is the DTG peak temperature, measured in degrees centigrade

mental analyses. The IR spectra contain a band at 922 cm^{-1}, assigned to asymmetric Mo–O vibrations [2, 8]. The band at 674 cm^{-1} could be assigned to the ν_s and ν_{as} Te–O stretching modes [2, 8]. The stretching band at 478 cm^{-1} was assigned to M–O, where *M*=Ni(II), Co(II) [8]. The deformation vibrations of the OH groups of the water molecules were observed at 1623 cm^{-1} [8]. The band at 3446 cm^{-1} was assigned to symmetric and asymmetric stretching vibrations of the OH groups of the water molecules [8].

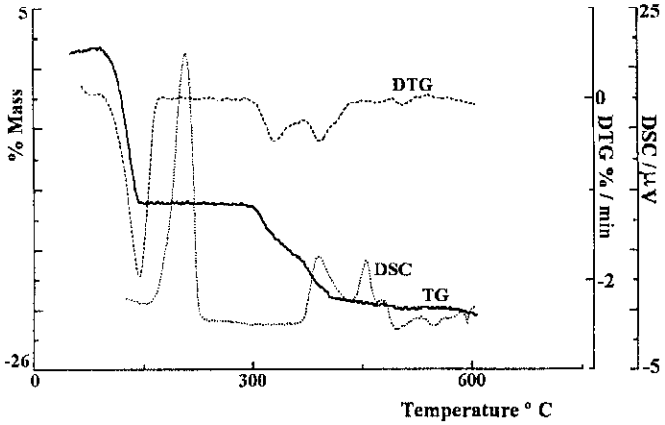

Fig. 1 TG, DTG and DSC curves at 5°C min^{-1} in dynamic dinitrogen atmosphere at 70 cm^3 min^{-1} for $[Ni(H_2O)_6]_3{\cdot}[TeMo_6O_{24}]$ (compound 1)

The second and third (overlapping) steps of the thermal decomposition for both compounds (Figs 1 and 2, respectively) correspond to an overall of 7 water molecules (calc. mass loss 9.0, found 8.5%) between 287 and 400°C for compound 1, and between 258 and 398°C for compound 2, according to the equation

$$[6MoO_3{\cdot}3MO{\cdot}TeO_3{\cdot}7H_2O]_{(s)} \rightarrow [6MoO_3{\cdot}3MO{\cdot}TeO_3]_{(s)} + 7H_2O_{(g)}$$

For this compound $[6MoO_3{\cdot}3MO{\cdot}TeO_3]$, the IR spectrum does not display bands corresponding to water molecules.

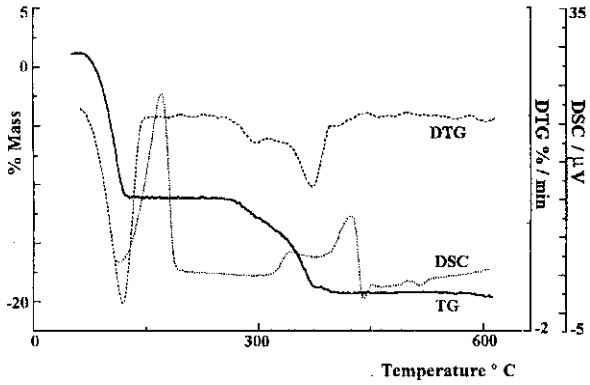

Fig. 2 TG, DTG and DSC curves at 5°C min^{-1} in dynamic dinitrogen atmosphere at 70 cm^3 min^{-1} $[Co(H_2O)_6]_3[TeMo_6O_{24}]$ (compound 2)

For the compound $Ni_3[TeMo_6O_{24}]\cdot 20H_2O$ [4], the water molecules are lost in two steps, up to 120°C (11 water molecules) and at 270°C (9 water molecules).

In the compounds described here, 7 water molecules are bonded more strongly than the former 11 water molecules. These 11 molecules are bonded only to cations (coordination water), whereas the remaining 7 are bonded both to cations (coordination water) and to anions by hydrogen-bonds, in accordance with the structures described in reference [6].

In the interval $400°C \leq T \leq 600°C$, yellow residual compounds were obtained for both compounds, which were characterized by IR and XPS. The XPS analysis revealed that the oxidation states for Mo and Te are 6, and those for Ni and Co are 2 [10].

The binding energy (BE) values for these elements in compounds 1 and 2 are listed Table 2. This Table demonstrates that there is a possibility for the formation of MoO_3, $NiMoO_4$, TeO_3, $NiTeO_4$ and NiO for compound 1, and MoO_3, $CoMoO_4$, TeO_3 and $CoTeO_4$ for compound 2.

In reference [4], the overall thermal decomposition of $[Ni_3[TeMo_6O_{24}]\cdot 20H_2O$ is described by the following equation:

$$2Ni_3[TeMo_6O_{24}]\cdot 20H_2 \rightarrow Ni_3TeMo_2O_{12}+3NiMoO_4+7MoO_3+TeO_2+1/2O_2+20H_2O$$

The conditions of thermal decomposition for $[Ni_3[TeMo_6O_{24}]\cdot 20H_2O$ [4] (DTA and TG under a vacuum of 10^{-5} mbar and a heating rate of 10°C min^{-1}) were very different from those described here, which explains why the residual products are different.

In the study of the kinetics of the process

$$[M(H_2O)_6]_3\cdot[TeMo_6O_{24}]_{(s)} \rightarrow [6MoO_3\cdot 3MO\cdot TeO_3\cdot 7H_2O]_{(s)}+11H_2O_{(g)}$$

where *M*=Ni(II), Co(II), under dynamic and isothermal conditions for both compounds, the results of the different models converged only for compound 2.

Table 2 Experimental and theoretical binding energies (*BE*) in eV, for elements in $[Ni(H_2O)_6]_3{\cdot}[TeMo_6O_{24}]$ (compound 1) and $[Co(H_2O)_6]_3{\cdot}[TeMo_6O_{24}]$ (compound 2)

Element	Binding energy (*BE*)/eV		
	experimental 400≤*T*(°C)≤600		theoretical [10]
	$[Ni(H_2O)_6]_3{\cdot}[TeMo_6O_{24}]$ (compound 1)		
$Mo_{3d5/2}$	232.5	MoO_3	232.6
		$CoMoO_4$	232.4
O_{1s}	530.6	MoO_3	530.4
		$CuMoO_4$	530.6
$Te_{3d5/2}$	576.5	TeO_3	576.6
		Na_2TeO_4	576.8
$Ni_{2p3/2}$	855.9	NiO	854.3
		Ni_2O_3	857.3
		$Ni(OH)_2$	855.6
	$[Co(H_2O)_6]_3{\cdot}[TeMo_6O_{24}]$ (compound 2)		
$Mo_{3d5/2}$	232.8	MoO_3	232.6
		$CoMoO_4$	232.4
O_{1s}	530.9	MoO_3	530.4
		$CuMoO_4$	530.6
$Te_{3d5/2}$	576.6	TeO_3	576.6
		Na_2TeO_4	576.8
$Co_{2p3/2}$	781.1	CoO	780.4
		Co_2O_3	779.9
		$CoMoO_4$	780.9

For compound 2, to study the kinetics of the above process, we recorded three curves in the dynamic regime at rates of 2, 5 and 8°C min^{-1}, and four on isothermal conditions at 60, 62, 64 and 66°C in a dynamic dinitrogen atmosphere. The initial and final temperatures and also the temperature of the peak of the derivative thermogravimetric curve (DTG) corresponding to the above-mentioned process are listed in Table 1.

To determine the possible model mechanism of the reaction, we used the formulae listed by Satava [11] (non-isothermal regime): one-dimensional diffusion: $g(\alpha)=\alpha^2$; two-dimensional diffusion, cylindrical symmetry: $g(\alpha)=\alpha+(1-\alpha)\ln(1-\alpha)$; three-dimensional diffusion, spherical symmetry (Jander equation): $g(\alpha)=[1-(1-\alpha)^{1/3}]^2$; three-dimensional diffusion, spherical symmetry (Ginstling-Brounshtein equation): $g(\alpha)=(1-2/3\alpha)-(1-\alpha)^{2/3}$; random nucleation, one nucleus on each particle: $g(\alpha)=-\ln(1-\alpha)$; random nucleation (Avrami equa-

tion 1): $g(\alpha)=[-\ln(1-\alpha)]^{1/2}$; random nucleation symmetry: $g(\alpha)=[-\ln(1-\alpha)^{1/3}$; phase boundary reaction, cylindrical symmetry: $g(\alpha)=1-(1-\alpha)^{1/2}$; and the Johnson-Gallagher equation $g(\alpha)=1/(1-\alpha)$ [12].

The best values of the regression coefficient, for fitting to a straight line using the least-squares method, correspond to one-dimensional diffusion; the equation $g(\alpha)=\alpha^2$ [11] gave the best mechanism for the reaction of loss of the water molecules (Table 3).

Table 3 Kinetic parameters and regression coefficients (*c*) calculated by assuming one-dimensional diffusion (O.D.D.), for the thermal dehydration of $[Co(H_2O)_6]_3\cdot[TeMo_6O_{24}]$ (compound 2)

	2°C min^{-1}, n=1.30			5°C min^{-1}, n=1.72			8°C min^{-1}, n=1.59		
	E_a	A	c	E_a	A	c	E_a	A	c
O.D.D.	163.4	$4.0\cdot10^{21}$	0.940	167.1	$5.4\cdot10^{21}$	0.966	168.5	$1.6\cdot10^{22}$	0.900

E_a in kJ mol^{-1} and A in s^{-1}

Kinetic parameters are very difficult to calculate merely from non-isothermal TG curves, due to ignorance of the true $g(\alpha)$ expression. It is necessary to compare the results obtained by non-isothermal and isothermal TG measurements for the expression $g(\alpha)=\alpha^2$ in order to calculate the true activation energy and to know the physical mechanism of the solid-state process. For this reason, we recorded not only the non-isothermal TG curves, but also the isothermal TG curves, at four different temperatures for compound 2.

Under isothermal conditions, we used the following general expression for the solid-state kinetic parameters:

$$g(\alpha)=\int_0^{\alpha}\frac{d\alpha}{dt}=kt+c$$

where $g(\alpha)$ is the expression of the physical model according to which the solid-state reaction is assumed to occur; the main expressions are presented in reference [11] (vide supra), α is the fraction decomposed at time t, and k is the rate constant of the process, related to the activation energy E_a, according to the Arrhenius expression:

$$g(\alpha)=\frac{A}{\beta}\int_0^{T}e^{-E/RT}dT$$

where A is the pre-exponential factor, β is dT/dt when the heating rate is constant, and R is the gas constant.

From the representation $g(\alpha)$ *vs.* t, the values of k are obtained. By applying the Arrhenius equation, it is possible to obtain E_a directly as the slope of the resulting $\ln[k(T)]$ *vs.* $1/T$ (E_a=167.4 kJ mol^{-1}), and the pre-exponential factor (A=2.7·10^{25} s^{-1}). In this way, an E_a value practically independent of the applied $g(\alpha)$ is obtained. The value obtained for E_a is in good agreement with that determined via the equation $g(\alpha)=\alpha^2$ (one-dimensional diffusion [11] by using dynamic methods (Table 3).

Since the values of k are known, we calculated the entropy $\Delta S^{\neq}$ and enthalpy of activation $\Delta H^{\neq}$ using the Eyring equation [13, 14]:

$$\ln\left(\frac{kh}{k_\beta T}\right)=\frac{\Delta S^{\neq}}{R}-\frac{\Delta H^{\neq}}{RT}$$

where k is the rate constant, h is the Planck constant, k_β is the Boltzmann constant, T is temperature, R is the gas constant and $\Delta S^{\neq}$ and $\Delta H^{\neq}$ are the entropy and enthalpy of activation, respectively.

By linear regression of $\ln(kh/k_\beta T)$ *vs.* $1/T$, we obtained $\Delta H^{\neq}$=89.2 kJ mol^{-1} and $\Delta S^{\neq}$=–36.7 J K^{-1} mol^{-1}, and the free energy of activation is $\Delta G^{\neq}_{336.15K}$ = 101.5 kJ mol^{-1}.

The value of E_a corresponds to a process with loss of water coordinatively bound to a cation [15].

According to House [16], the entropy effect may be explained in terms of the relative sizes of the atoms and the free volume; where there is a large space between the atoms, the water molecule may be able to slip into a position where it causes little or no lattice distortion, and the entropy of activation may therefore be negative, as in our case and in previous work on diazolium molybdotellurates [2, 3].

The calculated values of $\Delta H^{\neq}$ and $\Delta G^{\neq}$ are of the same order as those determined previously for other diazolium molybdotellurates [2, 3].

The computation for each function $g(\alpha)$ in the dynamic regime was carried out with the program CINEDAT [17].

Supplementary material

Kinetic data on compound 2 and XPS spectra of residual compounds 1 and 2 are available from the authors upon request.

* * *

P. G. gratefully acknowledges support from the Gobierno de Canarias (Project N° 689/94). Thanks are also due to Mrs. P. Agnew for correcting the English text.

References

1 M. J. Morris, Coord. Chem. Rev., 152 (1996) 309; 164 (1997) 289.
2 P. A. Lorenzo Luis, P. Martín-Zarza, A. Sánchez, C. Ruiz-Pérez, M. Hernández-Molina, X. Solans and P. Gili, Inorg. Chim. Acta, 277 (1998) 139.

3 P. A. Lorenzo Luis, P. Martín-Zarza, S. Domínguez, J. Manuel Arrieta, E. R. Castellón, J. J. Jiménez, A. Sánchez, C. Ruiz-Pérez, M. Hernández-Molina, X. Solans and P. Gili, Trans. Metal Chem., in press.
4 J. Sloczynski and B. Sliwa, Z. Anorg. Allg. Chem., 438 (1978) 295.
5 R. Grabowski, A. Gumula and J. Sloczynski, J. Phys. Chem. Solids, 41 (1980) 1027.
6 P. A. Lorenzo Luis, P. Martín-Zarza, R. Saez-Puche, E. R. Castellón, J. J. Jiménez, C. Ruiz-Pérez, J. González Platas, X. Solans and P. Gili, Eur. J. Solid State Inorg. Chem., 34 (1997) 1259.
7 A. C. Dengel, G. P. William, I. M. Sahar and A. J. P. White, Spectrochim. Acta, 49 (1993) 1583.
8 K. Nakamoto, Infrared and Raman Spectra of Inorganic and Coordination Compounds, 4th ed., 1986, p. 228.
9 J. E. Huheey, E. A. Keiter and R. L. Keiter, Inorganic Chemistry. Principles of Structure and Reactivity, 4th ed., Harper, 1993, p. 454.
10 J. F. Moulder, W. F. Stickle, P. E. Sobol and K. D. Bomben, Handbook of X-ray Photoelectron Spectroscopy, Perkin-Elmer Physical Electronics Division, 1992.
11 V. Satava, Thermochim. Acta, 2 (1971) 423.
12 D. W. Johnson and P. K. Gallagher, J. Phys. Chem., 75 (1971) 1179.
13 J. Rivas, A. Escuer, M. Serra and R. Vicente, Thermochim. Acta, 102 (1986) 125.
14 R. G. Wilkins, Kinetics and Mechanism of Reactions of Transition Metal Complexes, 2nd ed. VCH, Weinheim 1991, p. 88.
15 M. Hernandez-Padilla, S. Dominguez, P. Gili, A. Mederos and C. Ruiz-Perez, Polyhedron, 11 (1992) 1965.
16 J. E. House, Thermochim. Acta, 38 (1980) 59.
17 S. Dominguez and P. Gili, Program CINEDAT 1996. Departamento de Química Inorgánica, Facultad de Farmacia, Universidad de La Laguna, E-38200 Tenerife, Canary Islands, Spain.